Improved Electronic Interfaces for Heavy Loaded AT Cut Quartz Crystal Microbalance Sensors

Antonio Arnau, José V. García and Yolanda Jiménez
Departamento de Ingeniería Electrónica
Universidad Politécnica de Valencia
Valencia, Spain
aarnau@eln.upv.es

Vittorio Ferrari and Marco Ferrari
Dip. di Elettronica per l'Automazione and INFM
Università di Brescia
Brescia, Italy
vittorio.ferrari@unibs.it

***Abstract*— A new configuration of an automatic capacitance compensation (ACC) technique based on an oscillator-like working interface, which permits the tracking of the series resonant frequency, the monitoring of the motional resistance and the parallel capacitance of a thickness-shear mode (TSM) quartz crystal microbalance (QCM) sensor, is introduced. The new configuration permits an easier calibration of the system which, in principle, improves the accuracy. Experimental results are reported with 9 and 10MHz crystals in liquid with different parallel capacitances which demonstrate the effectiveness of the capacitance compensation. Some frequency deviations from the exact series resonant frequency, measured by an impedance analyzer, are explained by the specific non idealities of the circuit. A tentative approach is proposed to solve this problem that is also common to previous ACC systems.**

I. INTRODUCTION

In general, the following steps are involved in sensor applications: (a) measurement of the appropriate sensor parameters, (b) extraction of the corresponding physical parameters, related to the model selected for the specific application, starting from the measurements in the previous step, and (c) interpretation of the physical, chemical or biological phenomena which enable to explain the extracted parameters of the selected model. Step (a) is very important because an erroneous sensor parameter characterization can lead to a misinterpretation of the phenomena involved during the experiment. This problem occurs in thickness shear mode (TSM) microbalance sensors, when significant changes in the acoustic load or in the parallel capacitance of the sensor occur during the experiment, if appropriate electronic interfaces are not used. These effects are accentuated in the case of heavy acoustic loads and particularly happen when oscillators are used as quartz crystal microbalance (QCM) drivers [1].

The problem has been partially overcome by the development of oscillator-like operating feedback systems. These systems include both manual and automatic techniques to compensate the parallel capacitance of the sensor. In this way the series resonant frequency of the sensor is univocally determined at the zero-phase oscillating condition [2-5]. In this paper a new circuit configuration for automatic capacitance compensation (ACC) techniques, based on the same concept described elsewhere [4,5] is presented. The new configuration makes the calibration procedure easier and, in principle, improves its accuracy. A different approach for performing the capacitance compensation at high frequencies is introduced as well. Experimental results show the effectiveness of the capacitance compensation. However, some additional improvements are necessary to increase the accuracy of the system due to the non-ideal response of some components of the circuit. A new approach is proposed to avoid these inaccuracies.

II. THEORY

A loaded TSM quartz resonator sensor can be modeled around resonance by the lumped-element equivalent circuit shown in Fig.1.

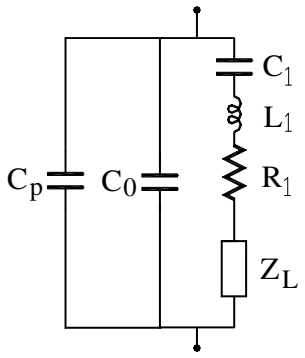

Figure 1. Lumped-element equivalent circuit of the sensor

The circuit is a generalization of the Butterworth-Van Dyke (BVD) model in which L_1, C_1, R_1 refer to the unperturbed sensor, C_0 is the so-called static capacitance of

This work was financed by the project PETRA II, ALFA II-0343-FA-FCD-FI, in the frame of ALFA program financed by the European Commission.

the crystal, C_p is the parasitic capacitance external to the sensor and Z_L is a complex impedance representing the contribution of the load. A detailed description of the relationships between the electrical parameters of the model and the physical and geometrical properties of the quartz crystal and the load can be found elsewhere [1]. For the purpose of this paper the model in Fig.1 is enough to show the problem of oscillators as drivers for QCM sensor characterization.

Oscillators' output frequency depends on the specific loop gain and phase oscillating conditions; therefore different oscillators can provide different output frequencies for the same experiment depending on the specific designed oscillating conditions. This effect which could not be easily recognized can lead to the risk of severe misinterpretations of the authentic frequency shift of the sensor characteristic frequency. The problem is qualitatively depicted in Fig.2. As it can be noticed, different frequency shifts, Δf_1 and Δf_2, would be provided by oscillators with different sensor phase oscillating conditions, α_1 and α_2, between two different instants of an experiment for which the conductance and phase responses of the sensor around the resonance are given by the plots 1, 1' and 2, 2' for instants 1 and 2 respectively. As it can be understood this effect is a consequence of the decrease of the steepness of the phase response of the sensor as a consequence of the damping effect due to the load. The conductance value of the sensor is also different at the two phase oscillating conditions, α_1 and α_2; this also implies an error in the characterization of the sensor damping when the conductance is taken as a parameter for its characterization.

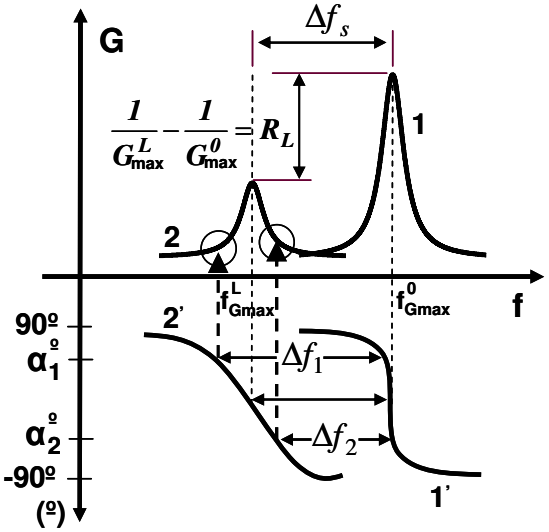

Figure 2. Problem of frequency monitoring in oscillators

The appropriate frequency and conductance to be monitored are those corresponding to the series resonance of the motional branch of the circuit in Fig.1, which are, for most cases, very close to those of the conductance peak of the sensor as shown in Fig.2 (f_{Gmax} and G_{max}). However, this point of the admittance response of the sensor is not univocally determined at a specific phase condition, $\Phi(f_{Gmax})$, that depends on both the total motional resistance R_T and the total parallel capacitance $C_0^*=C_0+C_p$ through (1). Therefore, a different strategy must be designed to continuously track this characteristic point.

$$\Phi(f_{Gmax})=\arctan[2\pi f_{Gmax} R_T C_0^*] \quad (1)$$

Fig. 3 shows, qualitatively, the typical locus of the admittance of a quartz sensor under different acoustic and dielectric loading. As it can be noticed, the high admittance zero-phase frequency, f_r, gives a good approximation of the maximum conductance frequency for low acoustic loads; however, when the acoustic load and/or the parallel capacitance increase the zero-phase frequency can not be longer considered as the maximum conductance frequency. On the contrary, if the parallel capacitance is compensated the zero-phase is the appropriate tracking condition for the maximum conductance monitoring.

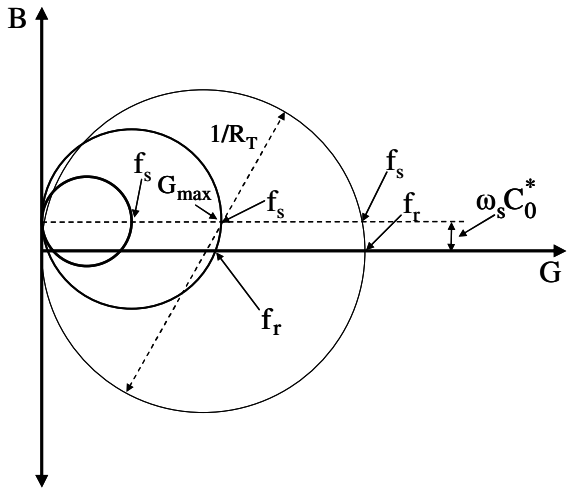

Figure 3. Typical admittance circle of a quartz crystal resonator for different loads.

III. CIRCUIT DESCRIPTION

The concept behind the design is the same introduced elsewhere [4], that is, by simultaneous exciting the quartz crystal at two frequencies, and assuming linear behavior of the resonator at the driving level of the signals, the compensation of the parallel capacitance, C_0^*, is automatically and simultaneously made with the locking of the series resonant frequency, f_s, of the sensor.

The new approach, shown in Fig.4, was partially introduced elsewhere [2] for manual capacitance compensation. In the present case two phase locked loops (PLL) are used for both frequency tracking and parallel capacitance compensation. The PLL in charge of the sensor series resonant frequency tracking is based on a phase-frequency detector (PFD) instead of a multiplier as it is the case in [4]. In this configuration the non inverter amplifier in charge of driving the sensor has, ideally, the same response at different frequencies inside its bandwidth of linear operation, since only a resistance, R_v, is included in the feedback loop unlike [4], where a resistance in parallel with a capacitance is

proposed to obtain a 90º phase-shift of the high frequency component of the composed driving signal, necessary for a proper operation of the multiplier as a phase detector (Fig.3 in [4]). Therefore, an easier and, in principle, a more accurate calibration of the PLL can be performed in this new configuration by following the procedure introduced elsewhere [2].

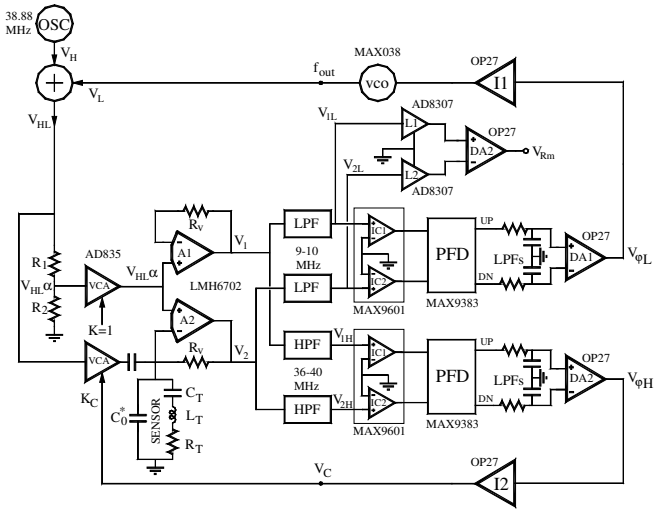

Figure 4. Block Diagrama of the ACC oscillator proposed.

A different approach is also followed in Fig.4 for the parallel capacitance compensation, where an auxiliary high frequency signal is used to perform the capacitance compensation. The frequency of this signal is selected around four times the fundamental resonant frequency of the sensor where only capacitive behavior of the crystal resonator is expected; only very small differences (less than 1% [6]) exist between the low frequency and high frequency capacitances of the sensor. In this new approach the parallel compensation is provided by a phase sensitive circuit similar to the one used for the frequency tracking, and the calibration of this loop can be performed easily and accurately in a similar way.

The magnitudes governing the operation of the system are the phase-shifts between the signals V_1 and V_2 at the two frequencies, f_H and f_L, corresponding in this case to the signal of fix frequency equal to 4-times the fundamental resonant frequency of the sensor and to the signal which sweeps the frequency around the series resonant frequency of the sensor, respectively. The phase-shift at the lower frequencies around the series resonant frequency of the sensor controls the PLL in charge of the frequency tracking, while the phase-shift at the auxiliary higher frequency controls the PLL in charge of the parallel capacitance compensation. Therefore, the equation governing the control of the system is:

$$V_{2HL} = \left[1 + R_v Y_T + j\omega R_v (C_0^* - C_c)\right] V_{1HL} \qquad (2)$$

where $V_{1HL} = V_{HL}\,\alpha$; $C_c = [K_C/\alpha - 1]$; $\alpha = R_1/(R_1+R_2)$; and $Y_T = [j\omega L_T + R_T + 1/j\omega C_T]^{-1}$.

The subindex *HL* in the previous equations means that the voltage waveform considered is the sum of the two sinusoidal signals V_H, with fix frequency f_H generated by the auxiliary oscillator whose frequency is around four times the fundamental resonant frequency of the sensor, and V_L with frequency f_L generated by the VCO around the series resonant frequency of the sensor.

At the auxiliary frequency, f_H, where only capacitive behaviour of the sensor is expected, (2) is reduced to:

$$V_{2H} = \left[1 + j\omega R_v (C_0^* - C_c)\right] V_{1H} \qquad (3)$$

and the phase shift between the signals V_{2H} and V_{1H} is given by:

$$\Phi(V_{2H}, V_{1H}) = \arctan[2\pi f_H R_v C_r] \qquad (4)$$

where $C_r = C_0^* - C_c$ is the residual uncompensated parallel capacitance.

As it can be noticed when $C_r = 0$ the phase shift is zero and the differential amplifier DA2 gives zero voltage at its output that makes the integrator I2 to maintain a continuously stable dc voltage at its output. This is the only stable condition for the loop out of saturation. In a different condition, $C_r \neq 0$, the amplifier DA2 gives a signal which is integrated by the integrator I2 until a new stable condition is reached for $C_r = 0$. The output V_C of the integrator I2 can be used to monitor the changes in the parallel capacitance of the sensor and also for a continuous monitoring of its magnitude.

The sensitivity of the capacitance compensation is limited by the sensitivity of the phase detector. Assuming a sensitivity of the phase detector of 0.1º, for the frequency f_H around 40 MHz and $R_v = 237\Omega$, the uncompensated residual capacitance obtained by solving C_r from (4) is near 30fF, which is enough for most cases.

At the frequency f_L, and assuming that the parallel capacitance has been compensated ($C_r = 0$), (2) is reduced to:

$$V_{2L} = \left[1 + R_v G_T + jR_v B_T\right] V_{1L} \qquad (5)$$

where $G_T = R_T/(R_T^2 + X_T^2)$; $B_T = -X_T/(R_T^2 + X_T^2)$ and $X_T = \omega L_T - 1/\omega C_T$

As it can be noticed from (5) signals V_{2L} and V_{1L} will be in phase when X_T is null and this only happens at series resonant frequency, $f_s = (2\pi L_T C_T)^{-1/2}$. At this frequency the differential amplifier DA1 gives a zero voltage at its output that makes the integrator I1 to maintain a continuously stable dc voltage at its output. This is the only stable condition for the loop out of saturation. If the series resonant frequency changes a phase shift between the signals will arise at the locked frequency and the amplifier DA1 will give a signal that will be integrated by the integrator I1 until a new stable condition is reached for the locking frequency at the new frequency f_s. It can be noticed

that the voltage at the input of the VCO can be used as a direct measurement of the shift in the series resonant frequency if the frequency range of the VCO is narrow enough to have good frequency/voltage sensitivity. A narrow bandwidth of the VCO can reduce the dynamic range of the PLL, however this can be avoided with the system described elsewhere [7].

At the series resonant frequency (5) is reduced to:

$$V_{2L} = \left[1 + \frac{R_v}{R_T}\right] V_{1L} \qquad (6)$$

and by measuring the voltage levels V_{2L} and V_{1L} the magnitude of the motional resistance R_T is obtained as explained elsewhere [2].

In the circuit in Fig. 4 the VCA connected to the output of the resistive divider formed by R_1 and R_2, is only included for symmetry.

IV. EXPERIMENTAL RESULTS

The circuit was implemented in a four-layer board by using the integrated circuits indicated in Fig. 4 and the following relevant component values: R_1=R_2=50Ω, R_v=237Ω, C = 18pF. The auxiliary frequency f_H was chosen around 38.88 MHz to be appropriate for 9 and 10 MHz quartz crystal resonators.

After the initial calibrations of the two loops by following the procedures indicated elsewhere [2], a preliminary characterization of the capacitance compensation was made by connecting different capacitors in the place of the sensor. The capacitors where measured by an impedance analyzer at the frequency f_H and their magnitudes compared with the extracted ones through the voltage V_C delivered by the system. The results are shown in Fig. 5; as it can be noticed there is a complete agreement between the capacitances measured by the impedance analyzer and those measured by the proposed system.

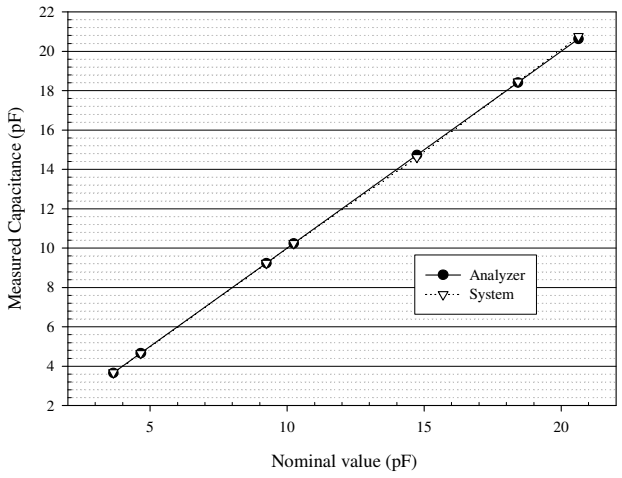

Figure 5. Capacitance characterization.

After the capacitance characterization, several experiments with 9 and 10 MHz sensors, one-face in contact with bi-distilled water, were performed. For each sensor external parallel capacitances of different magnitudes were added in order to check the effectiveness of the automatic parallel capacitance compensation of the system. If the automatic parallel capacitance were effective no changes in the locking frequency would be expected, since the parallel capacitance does not affect the series resonant frequency. The series resonant frequency of the sensor, one-face in contact with water, was previously measured, for each value of the added capacitor in parallel with the sensor, by measuring the corresponding maximum conductance frequency with an impedance analyzer; afterwards the locking frequency of the system was monitored in two different cases: without connecting the ACC loop and with the ACC loop connected. The results are shown in Figs. 6 and 7 for 9 and 10MHz quartz crystal respectively.

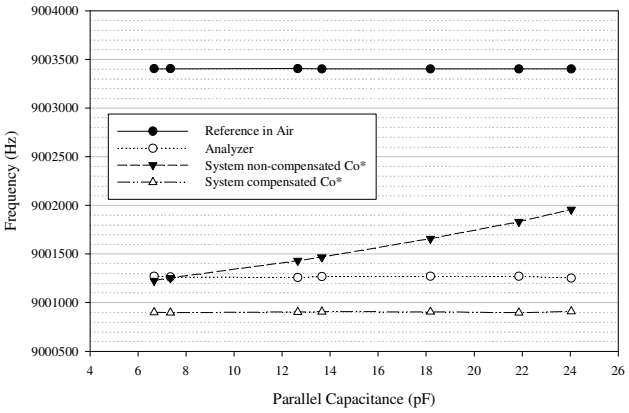

Figure 6. Measurements in water for a 9MHz sensor.

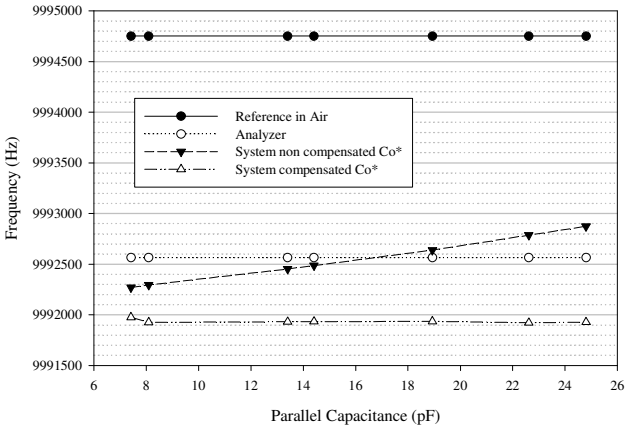

Figure 7. Measurements in water for a 10MHz sensor.

As it can be noticed, a change in the parallel capacitance can produce a change in the oscillating frequency of an oscillator working at zero-phase condition, as it is the case of the proposed system when the ACC loop is disconnected. However, there are no changes in the series resonant

frequency when a parallel capacitance is added to the sensor, as it can be noticed by the maximum conductance frequencies measured with the impedance analyzer. Then changes in the oscillating frequency of an oscillator can occur, even for non-heavy loads, when changes in the parallel capacitance occur during the experiment. When the ACC loop is connected the parallel capacitance is compensated and the looking frequency is maintained constant in all the cases, as it can be observed in Figs. 6 and 7 for both sensors. However a deviation between the maximum conductance frequency measured by the impedance analyzer and the frequency locked by the proposed system exists. This deviation is due to the different phase response between the non-inverter amplifier A2 and the amplifier A1 which is always working as a follower with gain 1 (Fig. 4). Effectively, the motional resistance measured by the system when the 9MHz sensor is one-face in contact with water is R_T=278MHz, therefore, according to (6) the gain of the non inverter amplifier is around 2. The different gain of the amplifiers has two effects, one is directly related to the different phase response, even for 9-10MHz, of the high bandwidth amplifiers, and the second one is due to the different amplitudes of the output voltages at V_{1L} and V_{2L} which, when compared in the comparators, are transferred into a phase error that is compensated by the system with a shift in the locking frequency.

This effect is corroborated in experiments made with heavy loads. After the experiments in water additional experiments with propylenglycol 99% and Glycerol 99% were made and the results are presented in Fig. 8. As it can be noticed the frequencies locked by the proposed system are apparently in good agreement with the maximum conductance frequencies measured by the impedance analyzer. However a more detailed analysis makes clear the effect of the different phase response of the amplifiers A1 and A2 for gains different from 1. Effectively, the relative errors, ε (%), between the measurements in liquid obtained by the impedance analyzer and by the system, in relation to the total frequency shift between the unperturbed state of the sensor and the sensor in contact with the liquids were calculated for the different liquids as indicated in (7) and represented in Fig. 8.

$$\varepsilon\,(\%) = \left[\frac{\left| f_{Anal.} - f_{Syst.} \right|_{liquid}}{f_{Air} - f_{liquid}} \right] \times 100 \qquad (7)$$

This error indicates that the relative deviations are much bigger in water than in the heavy liquids. In fact bigger errors would have been expected for heavy liquids than for water which does not represent a heavy load for the sensor. Furthermore, the ACC had to be necessarily included in the system with the sensor in contact with propylenglycol and glycerol, because no locking condition at zero-phase was found under these loading conditions without ACC. Moreover, deviations in water for 10MHz resonators (R_T=234Ω) were found to be bigger than for 9MHz resonators as it can be noticed in Figs. 6 and 7. This confirms that the effect of the phase response for different gains is increased with the frequency. The relative errors remained low, less than 4%, even for heavy loads as much as 5 KΩ of motional resistance which confirms the effectiveness of the ACC system.

The deviations for non heavy loads, like water, can be avoided by decreasing the value of the resistance R_v, or by designing a new strategy for an automatic gain control of the input stage of the system formed by the amplifiers A1 and A2. In the next paragraph a tentative approach is described for this purpose.

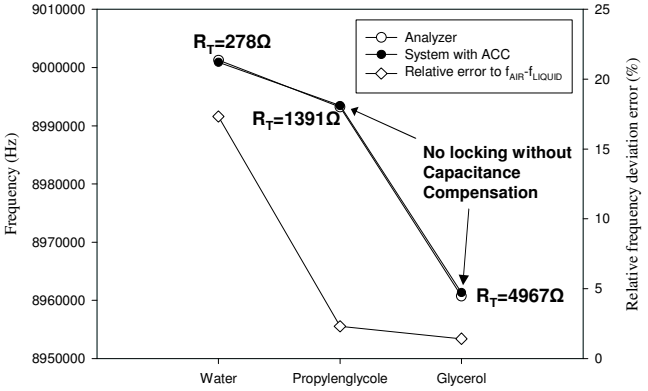

Figure 8. Measurements in water, propylenglycol and glycerol with a 9MHz sensor.

V. TENTATIVE APPROACH FOR FUTURE DEVELOPMENTS

Fig. 9 shows a tentative approach for an ACC system designed to control de gain of the amplifiers of the input stage to avoid the inconveniences described in the previous section.

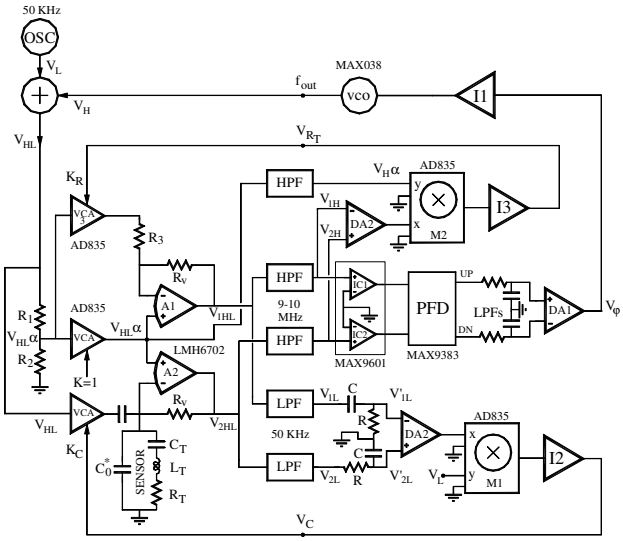

Figure 9. Tentative design for automatic gain control in ACC oscillators.

The loop in charge of the frequency locking has the same design previously described. In this approach the ACC is performed at low frequencies following the system described elsewhere [4], the reasons for making the ACC at low frequencies will be explained later on. Then the high frequency signals, V_H, in this approach, correspond to the

frequencies near the series resonant frequency, while the low frequency component, V_L, corresponds to the auxiliary low frequency signal used for parallel capacitance compensation (50 KHz).

The proposed configuration includes a new VCA with a resistance R_3 connected to the amplifier A1, which is converted into a non inverter amplifier. A new loop is included to control the gain, K_R, of the VCA3. The equation governing the new loop, assuming that the phases of the signals V_{1H} and V_{2H} are in phase and that the parallel capacitance is compensated is the following:

$$V_{2H} - V_{1H} = V_H \alpha R_v \left[\frac{1}{R_T} - \frac{1}{R_c} \right] \qquad (8)$$

where $R_c = R_3 / (1-K_R)$.

The integrator I3 maintains a stable dc output voltage for a zero voltage at its input. This condition, which is the only stable loop condition out of saturation, is only possible when the analog multiplier M2 provides zero voltage at its output. For signals $V_H \alpha$ and $V_{2H} - V_{1H}$ given by (8) at the inputs of the multiplier M2, the output provides zero voltage only for $R_T = R_c$. Under this condition the voltages V_{2H} and V_{1H} will have the same amplitude at the frequencies V_H and then the amplifiers A1 and A2 will work with the same equivalent gain at frequencies V_H. Moreover, the voltage V_{RT} at the output of the integrator I3 could be used as a direct measurement of the motional resistance R_T.

The automatic capacitance compensation in this new approach has to be made at low frequencies in order to avoid the different response of the amplifiers A1 and A2 at the auxiliary high frequency signal, proposed in the first configuration, for parallel capacitance compensation. Effectively, the conversion of the amplifier A1 in a non inverter amplifier, and the introduction of the resistance R_3, makes this amplifier to work with gains different from 1 at the selected auxiliary frequencies used for capacitance compensation, while amplifier A2 is working as a follower at these frequencies, once the parallel capacitance is compensated. The very different responses of these amplifiers at high frequencies, even multiples of the fundamental resonant frequency, is avoided at low frequencies where small differences in the gains of the input amplifiers have not relevant effects in their phase response.

VI. Conclusions

Oscillators can be used for fast frequency monitoring of quartz crystal resonator sensors, but the monitored frequency shifts can be erroneously identified with series resonant frequency shifts when changes in the parallel capacitance and/or in the sensor damping occur.

Automatic Capacitance Compensation Systems are a good alternative to oscillators for fast sensor characterization systems while providing a real-time monitoring of three parameters of interest: the series resonant frequency, the motional resistance and the change in the parallel capacitance of the sensor. This capability makes the ACC systems to be appropriate devices for experiments where changes in the properties of the medium imply a change in the parallel capacitance and/or in the quality factor of the sensor.

ACC systems can be easily calibrated without additional instrumentation and because the quartz crystal operates with one electrode tied to ground the ACC system is suitable for electrochemistry applications.

References

[1] A.Arnau Ed., Piezoelectric Transducers and Applications 1st ed., Chaps. 6 &12, Springer Verlag Berlin Heidelberg, 2004, pp.111-139 & 255-286

[2] A.Arnau, T.Sogorb, Y.Jiménez, "Circuit for continuous motional series resonant frequency and motional resistance monitoring of quartz crystal resonators by parallel capacitance compensation", Rev. Sci. Instrum., vol 73, 7, pp. 2724-2737, July 2002

[3] V. Ferrari, D. Marioli, A. Taroni, "Oscillator circuit configuration for quartz-crystal resonator sensors subject to heavy acoustic load", Electron. Lett., 36, 7, pp.610-612, 2000

[4] V. Ferrari, D. Marioli, A. Taroni, "ACC oscillator for in-liquid quartz microbalance sensors" Proc. IEEE Sensors 2003, vol 2, pp.849-854, 2003

[5] D. Rocha, V. Ferrari, and B. Jakoby, "Improved electronic readout circuit for resonant acoustic sensors," in Proc. IEEE Sensors 2004, vol 1, pp. 32–35, 2004

[6] W.G. Cady, Piezoelectricity (An introduction to the theory and applications of electromechanical phenomena in crystals). Dover, New York, 1964.

[7] R. Torres, A. Arnau, H. Perrot, J. García, and C. Gabrielli, "Analogue–digital phase-locked loop for alternating current quartz electrogravimetry" Electronics Letters, Vol 42, 22, October 2006, pp.1272-1273, 2006